



This discussion paper is/has been under review for the journal Hydrology and Earth System Sciences (HESS). Please refer to the corresponding final paper in HESS if available.

# Linking baseflow separation and groundwater storage dynamics in an alpine basin (Dammagletscher, Switzerland)

**F. Kobierska<sup>1,2</sup>, T. Jonas<sup>1</sup>, J. Kirchner<sup>3</sup>, and S. M. Bernasconi<sup>2</sup>**

<sup>1</sup>WSL Institute for Snow and Avalanche Research SLF, Davos, Switzerland

<sup>2</sup>Geological Institute, ETH Zurich, Sonneggstrasse 5, 8092 Zürich, Switzerland

<sup>3</sup>Department of Environmental Systems Science, ETH Zurich, Universitaetstrasse 22, 8092 Zürich, Switzerland

Received: 24 September 2014 – Accepted: 9 October 2014 – Published: 3 November 2014

Correspondence to: F. Kobierska (fbaffie@gmail.com)

Published by Copernicus Publications on behalf of the European Geosciences Union.

## Linking baseflow separation in an alpine basin

F. Kobierska et al.

[Title Page](#)

[Abstract](#)

[Introduction](#)

[Conclusions](#)

[References](#)

[Tables](#)

[Figures](#)



[Back](#)

[Close](#)

[Full Screen / Esc](#)

[Printer-friendly Version](#)

[Interactive Discussion](#)



## Abstract

This study aims at understanding interactions between stream and aquifer in a glacierized alpine catchment. We specifically focused on a glacier forefield, for which continuous measurements of stream water electrical conductivity, discharge and depth to the water table were available over four consecutive years. Based on this dataset, we developed a two-component mixing model in which the groundwater component was modelled using measured groundwater levels. The aquifer actively contributing to stream flow was assumed to be a superposition of two linear storage units. Calibrating the model against measured total discharge yielded reliable sub-hourly estimates of discharge and insights into groundwater storage properties. We found that a near-surface aquifer with high hydraulic conductivity overlies a larger reservoir with longer response time. Analyzing the mass balance of infiltration into the groundwater reservoir against exfiltration into the stream provided results that were in line with previous findings at this catchment.

## 1 Introduction

Groundwater storage dynamics in alpine catchments are difficult to determine, but could influence the response of mountain hydrology to climate change. A better understanding of stream-aquifer interactions is therefore necessary to predict hydrological flow patterns in the future. Alpine sites put additional constraints on data acquisition, as snow cover, weather conditions, and/or rough terrain limit the available measurements.

In this study, we estimate groundwater storage dynamics in the alpine headwater catchment fed by the Damma glacier in central Switzerland. In previous studies, we focused on local properties of the groundwater flow in specific stream reaches (Magnusson et al., 2014; Kobiarska, 2014). The aim is now to use this specific knowledge to upscale our hydrogeological understanding to the whole glacier forefield. We

**HESSD**

11, 12187–12221, 2014

### Linking baseflow separation in an alpine basin

F. Kobiarska et al.

[Title Page](#)

[Abstract](#)

[Introduction](#)

[Conclusions](#)

[References](#)

[Tables](#)

[Figures](#)



[Back](#)

[Close](#)

[Full Screen / Esc](#)

[Printer-friendly Version](#)

[Interactive Discussion](#)



seek to estimate the contribution of groundwater and hyporheic exchange to stream flow during different periods of the year, as well as the volume and response times of groundwater storage.

The topic of contributing storage to stream flow has been covered by many studies.

5 Analytical and numerical formulations of the Boussinesq equation (e.g. Brutsaert and Nieber, 1977; Rupp and Selker, 2006; Rupp et al., 2009) and linear or nonlinear reservoirs (e.g. Wittenberg and Sivapalan, 1999; Hannah and Gurnell, 2001; Majone et al., 2010) have been explored. At our site, traditional recession analysis is challenged by the fact that discharge is dominated by the diurnal dynamics of snow and glacier melt.  
10 Pure recession events are therefore very rare.

In alpine sites, mixing models based on natural tracers are a typical avenue for hydrograph separation (i.e. Hinton and Schiff, 1994; Liu et al., 2004; Covino and McGlynn, 2007; Blaen et al., 2013). Dzikowski and Jobard (2011) used electrical conductivity (EC) data to estimate the groundwater contribution to the discharge of an alpine  
15 stream. They defined seasonal envelopes rather than predicting groundwater flow and total flow for individual time steps. On the other hand, Covino and McGlynn (2007) presented groundwater table data but did not use them in their mixing model.

We suggest here a different approach to using mixing models, which involves a time-varying groundwater input. We implemented a two-component mixing model (glacier melt and groundwater) in which the groundwater exfiltration component is the output of two superposed linear groundwater reservoirs. A variable reservoir volume was computed using five groundwater stage measurements (referred to as “GW stage data”) throughout the forefield. In the following, we refer to infiltration as the flow from the  
20 stream into the aquifer and to exfiltration as the flow of groundwater and hyporheic exchanges back into the stream.  
25

To verify the robustness of the model and to understand the influence of each data input taken separately (EC or GW stage data), we compared our calibrated model to two benchmark models each forcing electrical conductivity or groundwater level to remain constant. By further analyzing groundwater interactions (infiltration and exfiltration) with

## Linking baseflow separation in an alpine basin

F. Kobierska et al.

[Title Page](#)

[Abstract](#)

[Introduction](#)

[Conclusions](#)

[References](#)

[Tables](#)

[Figures](#)



[Back](#)

[Close](#)

[Full Screen / Esc](#)

[Printer-friendly Version](#)

[Interactive Discussion](#)



stream water, we: (1) verify that groundwater exfiltration estimates are realistic, (2) estimate the volume of the active groundwater storage and (3) conclude with a conceptual representation of the forefield's main hydrogeologic features.

## 2 Study site and experimental methods

### 2.1 Site description

The Damma glacier forefield (Fig. 1) is part of a small (10.7 km<sup>2</sup>) granitic catchment situated in the central Swiss Alps. It is currently being studied as part of the SoilTrEC project (Bernasconi et al., 2011). The glacier covers 40 % of the catchment and has been retreating since the end of the Little Ice Age (LIA). Due to a sharp change in gradient, a small piece of glacier has become detached from the main glacier during its retreat and is referred to as the “dead ice body”. Large lateral moraines date from approximately 1850 (the end of the LIA) and two terminal moraine bands dating from 1927 and 1992 mark the end of two short periods of re-advance. The elevation of the catchment ranges from 1800 to 3600 m a.s.l. and the entire catchment is covered by snow for approximately six months per year.

The glacier forefield itself ranges from 1800 to 2000 m a.s.l. and covers an area of approximately 0.5 km<sup>2</sup>. The average annual temperature is 2.2 °C at the forefield. In 2008, annual precipitation and evapotranspiration for the whole catchment were estimated at 2300 and 70 mm respectively (Kormann, 2009). With a yearly cumulative discharge of approximately 2700 mm, the water balance of the catchment is clearly positive and corresponds to an average glacier mass loss of about one meter depth per year.

The basin is characterized by heavy snowfall in winter, making discharge difficult or impossible to measure. Discharge becomes dominated by baseflow as snow and glacier melt gradually cease in late autumn. In late spring (typically end of May), snowmelt leads to a strong increase in discharge and a clear daily cycle is quickly

## Linking baseflow separation in an alpine basin

F. Kobierska et al.

Title Page

Abstract

Introduction

Conclusions

References

Tables

Figures



Back

Close

Full Screen / Esc

Printer-friendly Version

Interactive Discussion





forefield (Kobierska, 2014). The results suggest that the saturated glacial till should be at least 10 m thick in much of the forefield, including in the vicinity of the discharge station. An important passive aquifer can therefore be expected in the forefield.

## 2.2 Hydrometeorological data

5 Groundwater levels were measured with Hobo U20 Water Level Loggers (5 min sampling interval averaged to 30 min values) at S1, S3, S5 and S6 as shown in Fig. 1. The method is described in detail in Magnusson et al. (2014). Stream stage was measured at the catchment outlet (S7 in Fig. 1), using both a cable-supported radar device and a pressure logger installed in a partly perforated tube. The rating curve of discharge as a function of stream level was calibrated with the results of salt and dye tracer dilution tests across a wide range of flows ( $35$  to  $4500 \text{ L s}^{-1}$ , see Magnusson et al., 2012 for further details).

10 Table 1 presents values of the main hydro-meteorological parameters for successive winters and summers (taken from start of June to end of October), as measured by the discharge station and the meteorological station (S7 and AWS in Fig. 1). This highlights the succession of hydro-climatically different years, which presented a good opportunity to test the robustness of the model.

15 For example, Table 1 shows large year-to-year variability in snow water equivalent (SWE) and annual rainfall, and also shows that neither water source strongly dominates the water balance. Snow water equivalent (SWE) was estimated from the maximum snow depth of each winter, assuming a density of 0.3. Cumulated rainfall is the raw data measured at the AWS. Note that both SWE and rainfall data were measured in the forefield and are thus not representative of the water input to the whole catchment which extends 1800 m above the forefield. Cumulated discharge also contains a significant ice melt component, which was not estimated in this study.

## Linking baseflow separation in an alpine basin

F. Kobierska et al.

Title Page

Abstract

Introduction

Conclusions

References

Tables

Figures



Back

Close

Full Screen / Esc

Printer-friendly Version

Interactive Discussion



## 2.3 Electrical conductivity endmembers

EC and temperature were measured at the main runoff station (S7) with a WTW Tetracon 325 sensor (accuracy 0.5 % for EC, 0.5 °C for temperature under 15 °C). The 10 min sampling rate was averaged to 30 min values for this study. Various measurements of groundwater springs were also carried out throughout the forefield with a hand-held WTW Cond 315i device (same accuracy) in order to determine endmember values for use in the mixing model. Continuous EC measurements of groundwater and streamwater are also available for summer 2011 at three transects (S1, S3 and S5) and at some springs between S5 and S0. EC was temperature-corrected using a non-linear correction to a reference of 20 °C.

From those measurements, an electrical conductivity map of the forefield can be sketched (Fig. 1) with 6 geographically distinct areas (all displayed in Fig. 6). Between 2009 and 2012, EC measured at the main runoff station (S7) varied from 2 to 13.3  $\mu\text{S cm}^{-1}$  with an average value of 6.6  $\mu\text{S cm}^{-1}$ . The main section of the stream through the forefield is fed by two glacial sub-catchments of low EC (areas L1 and L2, lower end only). Direct measurements of glacier melt on the dead ice body yielded EC values ranging from 1.7 to 2.1  $\mu\text{S cm}^{-1}$ . We use the lowest EC value measured for melting ice (1.7  $\mu\text{S cm}^{-1}$ ) as the endmember value for glacier melt. EC can be assumed to be a conservative tracer in open-channel flow because of the short travel time of surface runoff through the forefield (on the order of 10 min). This is confirmed by the low EC values (minimum of 2  $\mu\text{S cm}^{-1}$ ) measured at the discharge station during extreme flow events.

Three distinct zones are rich in springs (areas H1, H2 and H3) and consistently present conductivities between 13 and 18  $\mu\text{S cm}^{-1}$  (Table 1). Those groundwater exfiltration zones average 15.1  $\mu\text{S cm}^{-1}$  and show very little temporal variability, as witnessed by continuous data-logger measurements for summer 2011 in the upper part of H1. We can therefore confidently attribute an endmember value of approximately 15.1  $\mu\text{S cm}^{-1}$  to groundwater exfiltration in the forefield.

## Linking baseflow separation in an alpine basin

F. Kobierska et al.

Title Page

Abstract

Introduction

Conclusions

References

Tables

Figures



Back

Close

Full Screen / Esc

Printer-friendly Version

Interactive Discussion



### 3 Models

#### 3.1 Two-component mixing model

In the previous section, we found that EC displayed two distinct endmembers: ground-water at  $15.1 \mu\text{S cm}^{-1}$ , and glacier melt at  $1.7 \mu\text{S cm}^{-1}$ . As stream water EC was consistently anti-correlated to runoff, we considered using mixing models to study the relationship between EC and discharge at the basin scale.

Our modelling approach requires a set of specific assumptions:

1. the EC measured at the main discharge station is the result of pure mixing between glacier melt and groundwater exfiltration into the stream.
2. glacier melt has a constant EC of  $\text{EC}_{\text{gl}} = 1.7 \mu\text{S cm}^{-1}$  (the lowest EC value measured for melting ice on the dead ice body).
3. exfiltrating groundwater has a constant EC of  $\text{EC}_{\text{gw}} = 15.1 \mu\text{S cm}^{-1}$  (average of all groundwater measurements).

The first assumption of pure two-component mixing is violated when rain falls. Several rain events affected both discharge and EC signals during the study period. Because quantifying rainfall throughout the forefield and its impact on stream water EC was not the aim of this study, data was removed when more than two millimeters of cumulated rain had fallen in the last five hours. This filter was designed to neglect the direct increase in surface runoff but not the subsequent exfiltration of rainwater that had infiltrated the aquifer. The filter threshold of 2 mm per 5 h is similar to typical melt rates, and led to removing 10.8% of the data. The deleted time periods can be seen as gaps in the EC data (upper panel of Fig. 3).

The second assumption is best met in midsummer when melt water runoff is dominated by glacier melt. The model does not differentiate snowmelt from glacier melt, as the same low endmember value  $\text{EC}_{\text{gw}}$  is used.

## HESSD

11, 12187–12221, 2014

### Linking baseflow separation in an alpine basin

F. Kobierska et al.

Title Page

Abstract

Introduction

Conclusions

References

Tables

Figures



Back

Close

Full Screen / Esc

Printer-friendly Version

Interactive Discussion



Finally, continuous EC measurements at several groundwater springs have shown that EC is reasonably constant in time (previous section), justifying our third assumption. In summary, the assumptions can be written as follows:

$$Q(t) = Q_{\text{gw}}(t) + Q_{\text{gl}}(t) \quad (1)$$

$$Q(t) \cdot \text{EC}(t) = Q_{\text{gw}}(t) \cdot \text{EC}_{\text{gw}} + Q_{\text{gl}}(t) \cdot \text{EC}_{\text{gl}} \quad (2)$$

where  $Q(t)$  is total discharge at time  $t$ ,  $\text{EC}_{\text{gw}}$  and  $\text{EC}_{\text{gl}}$  are respectively the groundwater and glacier electrical conductivity endmember values, and  $Q_{\text{gw}}(t)$  is the groundwater exfiltration flow which will be presented in the previous section. Equations (1) and (2) then yield Eq. (3):

$$Q(t) = \frac{(\text{EC}_{\text{gw}} - \text{EC}_{\text{gl}}) \cdot Q_{\text{gw}}(t)}{\text{EC}(t) - \text{EC}_{\text{gl}}} \quad (3)$$

## 3.2 Groundwater exfiltration model

### 3.2.1 Slow linear reservoir

Preliminary simulations with a nonlinear storage model were difficult to optimize due to equifinality problems. We therefore decided to superpose a “slow” and a “fast” linear reservoir, to respectively account for: (1) a baseflow component contributing to slow drainage of the aquifer in winter, and (2) a daily variable part resulting from near-surface interactions with the stream. The “fast” reservoir was set up to start filling only when the “slow” reservoir is full. The “slow” reservoir then remains constant and does not account for increased hydraulic head as the “fast” reservoir fills up. For both reservoirs, groundwater exfiltration is a linear function of storage volume as in Eq. (4):

$$Q_{\text{gw}}(t) = \frac{V(t)}{T} \quad (4)$$

where the proportionality factor  $T$  is the response time constant of the reservoir ( $T_{\text{slow}}$  or  $T_{\text{fast}}$ ) and  $V(t)$  is the volume of the reservoir at each time step ( $V_{\text{slow}}$  or  $V_{\text{fast}}$ ).

Recession techniques (i.e. Brutsaert and Nieber 1977; Wittenberg and Sivapalan, 1999) could not be applied during the main season at our site due to the variable glacier melt input throughout the hydrological season. In autumn, glacier melt progressively decreased and eventually stopped in winter. However, reliably measuring discharge in winter was difficult due to environmental constraints (i.e. snow load, icing in the river channel). Pure recession events with reliable data were therefore rare at this site.

We calibrated  $T_{\text{slow}}$  with a recession event at the end of 2008, which was the only long and clean discharge recession available during the four-year study period. This year was marked by an early big snow storm after which snow cover persisted into winter. Snow covered the whole forefield but had no effect on the stream geometry, such that the subsequent stage measurements were not affected by snow loads. Pure recession was established as the thick snow cover was efficient in stopping glacier and snow melt, even through some short warm periods that followed.

### 3.2.2 Fast linear reservoir

A total of nine groundwater level sensors and four stream stage sensors were installed in the forefield and could be used to compute a groundwater storage function. To best describe average water table fluctuations in the forefield, only the five tubes furthest away from the stream were used ( $S1_{\text{far}}$ ,  $S3_{\text{far}}$ ,  $S5_{\text{far}}$ ,  $S6_{\text{far}}$  and  $S0$ ). From mid-October onwards, most tubes were usually empty except  $S6_{\text{far}}$  which some years provided stage data until December. For this reason and because there were other periods during which data from some tubes were missing, we computed the reservoir function as an integral of mean stage variations. For each time step, the integral water level in the reservoir  $L_{\text{integral}}$  was implemented as follows:

$$L_{\text{integral}}(t) = L_{\text{integral}}(t - \Delta t) + \sum_{i=\text{tubes}} \frac{L_i(t) - L_i(t - \Delta t)}{i} \quad (5)$$

12196

## Linking baseflow separation in an alpine basin

F. Kobierska et al.

Title Page

Abstract

Introduction

Conclusions

References

Tables

Figures

⏪

⏩

◀

▶

Back

Close

Full Screen / Esc

Printer-friendly Version

Interactive Discussion





### 3.3 Model calibration and performance assessment

#### 3.3.1 Calibrating against total discharge

The model was calibrated separately during each full hydrological year that was available (2009 to 2012 included) and validated with the remaining years. Calibration started at the beginning of June and stopped when EC became unavailable, usually mid-October. Relative error was used as a performance measure for calibration. In addition, the Nash-Sutcliffe efficiency (NSE) and benchmark efficiency (BE) were evaluated based on Eq. (7):

$$\text{Efficiency} = 1 - \frac{\sum_t (Q_{\text{meas}}(t) - Q_{\text{mod}}(t))^2}{\sum_t (Q_{\text{meas}}(t) - Q_{\text{bench}}(t))^2} \quad (7)$$

where  $Q_{\text{meas}}$  is measured discharge;  $Q_{\text{mod}}$  is modelled discharge and  $Q_{\text{bench}}$  is either runoff predicted by a benchmark model (to compute the BE) or by the average of the measured data (to compute the NSE). Our benchmark model uses the discharge value recorded exactly 24 h earlier, which is a rather stringent test as the signal displays daily fluctuations for much of the hydrological season. Due to the high-amplitude seasonal discharge record, the average measured discharge poorly describes the catchment hydrology. For this reason, BE provides a better assessment of model performance than NSE, which is bound to be high.

Two alternative models (named partial models thereafter) were tested against the full model, each of which used only one type of field measurement (either EC or GW). The aim was to determine whether including both electrical conductivity and groundwater data improved the accuracy of the model.

The first partial model, denoted  $P_{\text{EC}}$ , used Eq. (3) with a calibrated constant groundwater exfiltration rate ( $Q_{\text{gw}}$ ). Weijs et al. (2013) used this model to calibrate a rating curve using EC rather than stream stage. The second partial model, denoted  $P_{\text{GW}}$ , had

## Linking baseflow separation in an alpine basin

F. Kobierska et al.

Title Page

Abstract

Introduction

Conclusions

References

Tables

Figures



Back

Close

Full Screen / Esc

Printer-friendly Version

Interactive Discussion



a variable groundwater inflow as per Eq. (6) but used a constant value for EC (yearly average).

### 3.3.2 Infiltration and exfiltration properties

Equation (4) for the “fast” reservoir allows parameter  $T_{\text{fast}}$  to compensate a reservoir of inadequate volume  $V_{\text{fast}}$ . This creates an equifinality problem for the calibration routine. In an attempt to constrain the maximum volume of the fast reservoir, we calculated groundwater infiltration from the stream into the aquifer. The sum of this infiltration term and of the groundwater exfiltration back into the stream represents all the exchanges between stream and aquifer. Neglecting evapo-transpiration, we can write the mass balance of the storage volume  $V$  for the infiltration rate  $Q_{\text{inf}}$  as Eq. (8):

$$Q_{\text{inf}}(t) = \frac{dV(t)}{dt} + Q_{\text{gw}}(t). \quad (8)$$

Equation (8) can provide an upper limit to the reservoir volume (multiplying constant  $A_{\text{fast}}$  in Eq. 6), as infiltration rates may not become negative. Additionally, using Darcy’s Law and Eq. (8), the exchange surfaces  $A_{\text{inf}}$  and  $A_{\text{exf}}$  required to respectively infiltrate  $Q_{\text{inf}}$  and exfiltrate  $Q_{\text{gw}}$  can be written as follows:

$$A_{\text{inf}}(t) = \left[ \frac{dV(t)}{dt} + Q_{\text{gw}}(t) \right] \cdot \frac{1}{K_{\text{sat}}} \quad (9)$$

$$A_{\text{exf}}(t) = \frac{Q_{\text{gw}}(t)}{G_{\text{exf}} \cdot K_{\text{sat}}} \quad (10)$$

where  $K_{\text{sat}}$  is the saturated hydraulic conductivity and  $G_{\text{exf}}$  the average exfiltration gradient. Equation (9) assumes vertical infiltration through saturated soil. Based on previous experimental work at this site (Kobierska et al., 2014),  $K_{\text{sat}}$  was set to  $10^{-3} \text{ m s}^{-1}$ . The hydraulic gradient was assumed vertical where groundwater infiltrates. The gradient  $G_{\text{exf}}$  forcing the exfiltration component is difficult to evaluate due to the heterogeneous

## Linking baseflow separation in an alpine basin

F. Kobierska et al.

Title Page

Abstract

Introduction

Conclusions

References

Tables

Figures

⏪

⏩

◀

▶

Back

Close

Full Screen / Esc

Printer-friendly Version

Interactive Discussion



surface topography and the complex shape of the river bed. Topographic gradients vary roughly between 0 and 20 % in the forefield, so we tested two intermediate options with 5 and 15 %.

Finally, assuming that the entire width of the stream bed interacts with the aquifer (i.e. is either involved in infiltration or exfiltration), the stream width required for those exchanges can be estimated with Eq. (11):

$$\text{width}_{\text{stream}} = \frac{\left[ \frac{dV(t)}{dt} + Q_{\text{gw}}(t) \cdot \left( 1 + \frac{1}{G_{\text{exf}}} \right) \right] \cdot K_{\text{sat}}^{-1}}{\text{length}_{\text{stream}}} \quad (11)$$

where  $\text{length}_{\text{stream}}$  is the length of stream where those groundwater exchanges take place. We excluded the side stream (see zone L2 in Fig. 1) and set  $\text{length}_{\text{stream}}$  to 1000 m, which is the length of the forefield including the “dead ice body”.

## 4 Results

### 4.1 Slow reservoir properties

The month of November 2008 presented the only pure recession event lasting more than two weeks with reasonable discharge amplitude. In all other years, continuous measurements ended too early due to disturbances from snow loads and icing in the river channel. Based on Eq. (4), the recession hydrograph can be fitted using Eq. (12):

$$Q_{\text{recession}}(t) = Q_{\text{meas}}(t_{\text{end}}) \cdot \exp\left(\frac{(t_{\text{end}} - t)}{T_{\text{slow}}}\right) \quad (12)$$

where  $Q_{\text{meas}}(t_{\text{end}})$  is the measured discharge at the end of the recession event and  $Q_{\text{recession}}(t)$  is the modelled discharge at any time before the end of the measured

Title Page

Abstract

Introduction

Conclusions

References

Tables

Figures

⏪

⏩

◀

▶

Back

Close

Full Screen / Esc

Printer-friendly Version

Interactive Discussion



event ( $t_{\text{end}}$ ). This method has the advantage of not requiring an exact knowledge of when the recession event started, and yields a value of 29 days for  $T_{\text{slow}}$ .

As illustrated by the use of a logarithmic axis in Fig. 2, the linear fit with the recession data was very good from 15 November to the end of the record. Substantial snowfall occurred between 28 and 31 October, bringing snow depth at the meteorological station from 0 to 113 cm. Between the last peak discharge (5 November) and mid-November, a rain on snow event occurred, which prevented total discharge from only representing baseflow. The entire catchment remained covered by snow and on the 11 November, as the air temperature sharply dropped below  $0^{\circ}\text{C}$ , water percolation through the snow-pack stopped. Soil moisture in the upper soil layers subsequently dropped indicating the start of pure baseflow recession. The good recession fit starting shortly after this date shows that the linearity of the reservoir was a plausible assumption.

Based on the assumptions formulated in the Methods Section regarding the superposition of the “slow” and “fast” reservoirs, the maximum value of the modelled recession fitting with measured discharge is denoted baseflow $_{\text{max}}$ , with a value of  $0.07\text{ m}^3\text{ s}^{-1}$  (Fig. 2, lower panel).

## 4.2 Model calibration against total discharge

Figure 3 shows the model results for 2009. Daily variations in total discharge are appropriately reproduced, although with some underestimation in early summer (zoom 1). Discharge recessions following two cold snaps around 20 June and 10 July are however accurately modeled. The modelling results significantly improve from the beginning of August onwards (zooms 2 and 3), as non-glaciered slopes have become snow free.

Those results were obtained with the area of the “fast” reservoir  $A_{\text{fast}}$  set to 1000 m by 100 m. This seems a reasonable value as infiltration remains positive throughout the season except after a heavy rain event at the end of the record. In zooms 1, 2 and 3, daily cycles of infiltration and exfiltration dominance (day and night, respectively) are apparent. The size of the “fast” reservoir will be further considered in the discussion.

### Linking baseflow separation in an alpine basin

F. Kobierska et al.

Title Page

Abstract

Introduction

Conclusions

References

Tables

Figures



Back

Close

Full Screen / Esc

Printer-friendly Version

Interactive Discussion



---

**Linking baseflow  
separation in an  
alpine basin**F. Kobierska et al.

---

[Title Page](#)[Abstract](#)[Introduction](#)[Conclusions](#)[References](#)[Tables](#)[Figures](#)[⏪](#)[⏩](#)[◀](#)[▶](#)[Back](#)[Close](#)[Full Screen / Esc](#)[Printer-friendly Version](#)[Interactive Discussion](#)

The cross-validation results of the four years of data are presented in Table 3. Both partial models ( $P_{EC}$  and  $P_{GW}$ ) were tested, and displayed worse performance in all cases. This finding reveals that including both electrical conductivity and groundwater level data benefited the full model. Of the two data sources used in the full model, EC provides better information for modelling discharge, as model  $P_{GW}$  performed much worse than model  $P_{EC}$ .

The optimal parameter  $T_{fast}$  was 6.5 h. Our model presents reliably good performance, which suggests that the main assumptions may be consistent with the physical processes involved.

### 4.3 Verifying exfiltration and infiltration

The aim of this section is to use complementary methods to verify whether modeled groundwater exchange rates were realistic. Based on Eq. (11) and constant values that were chosen in the Methods Section ( $K_{sat}$  and  $L_{stream}$ ), the required stream width for  $4 \text{ m}^3 \text{ s}^{-1}$  of discharge ranges from 5 to 14 m for a hydraulic gradient varying between 15 and 5 %.

The complex braided nature of the stream through the forefield makes it difficult to measure its average width. On a 400 m long stream reach between S3 and S6, Magnusson et al. (2012) suggested a stream width of 24 m for  $4 \text{ m}^3 \text{ s}^{-1}$  of discharge. Their results, based on a completely different method (stream temperature analysis), are within the same order of magnitude as our estimates. As our modelled stream width is a function of groundwater exfiltration, this suggests that this mixing component was well parameterized and that our model may capture water exchanges in the forefield in a physically realistic manner.

Figure 4 shows the estimated percentage of groundwater exfiltration as a function of total measured discharge for 2009. Only the best modelled time steps are displayed (less than 10 % absolute error in total discharge). The season starts with medium flow and a high groundwater contribution (snowmelt-dominated in June), then progresses to high flows with a very low groundwater contribution (glacier-melt-dominated in August).

The end of the season (September) is characterized by low flows and an increasing groundwater contribution. Those qualitative results suggest that the model is appropriately describing exfiltration processes.

#### 4.4 Verifying $A_{\text{slow}}$ with spring recharge

The maximum volume of the “slow” reservoir can be estimated with Eq. (4), using the optimal parameter  $T_{\text{slow}}$  presented earlier ( $T_{\text{slow}} = 29$  days) and the baseflow $_{\text{max}}$  value of  $0.07 \text{ m}^3 \text{ s}^{-1}$ . For 1000 m of length and 400 m of width, this yields a maximum depth of 1.73 m. The surface of the aquifer was assumed based on topographical data (see Fig. 1) and perceptual understanding of the forefield. Porosity was set to 0.25, the average of all sites mentioned in Smittenberg et al. (2011).

The aim of Fig. 5 is to illustrate the recharge of the slow reservoir during spring snow melt. Using Eq. (4) to relate the volume of water in the reservoir ( $V_{\text{slow}}(t)$ ) and its exfiltration rate ( $Q_{\text{gw}}(t)$ ), and adding a recharge term  $R(t)$ , the volume function can be expressed as follows:

$$V_{\text{slow}}(t) = V_{\text{slow}}(t - \Delta t) + \left( R(t) - \frac{V_{\text{slow}}(t - \Delta t)}{T_{\text{slow}}} \right) \times \Delta t \quad (13)$$

where  $\Delta t$  is the time step (30 min in our case).

After a 150 day period with little or no recharge (November to end of March), the slow reservoir would come out of winter with only 10 cm storage remaining. In Fig. 5, the recharge of the reservoir was simulated using Eq. (13) with a recharge rate of  $100 \text{ L s}^{-1}$  during every snowmelt period. This rate is equivalent to complete infiltration of  $22 \text{ mm day}^{-1}$  of snowmelt in the forefield. Even though  $S6_{\text{far}}$  fills at an early date, for the following interpretation, we retain the conceptual view that the “fast” reservoir starts filling once the “slow” reservoir is full.

The main feature of Fig. 5 is the successive appearance of permanent water in the different groundwater tubes (plotted GW levels are the depth of water in each tube).  $S6_{\text{far}}$  is located at the lower end of the forefield and is quickly filled by permanent water.

## Linking baseflow separation in an alpine basin

F. Kobierska et al.

Title Page

Abstract

Introduction

Conclusions

References

Tables

Figures

⏪

⏩

⏴

⏵

Back

Close

Full Screen / Esc

Printer-friendly Version

Interactive Discussion





empty by the end of the season (end of October) when the “fast” reservoir has depleted. Based on this depth, the simulations in Fig. 3 were carried out with a “fast” reservoir area ( $A_{\text{fast}}$ ) of 1000 by 100 m. This corresponds to the length of the forefield by twice the distance from the stream to S0, and is also roughly the average width of the braided river system over the forefield (slightly smaller than the green zone in Fig. 6).

Based on those geometrical aspects, we suggest that the “fast” aquifer is characterized by high hydraulic conductivities (in the order of  $10^{-3} \text{ m s}^{-1}$ ), spans the riparian and hyporheic zone of the braided stream network and is on the order of one meter deep.

## 5.2 Conceptual hydrogeological model of the forefield

The aim of this section is to propose a conceptual overview of the site’s hydrogeology, based on modelling insights and previous results. This is illustrated by Fig. 6.

The modelling chain presented in this study yielded robust simulation of total discharge as a function of groundwater levels in the forefield and stream EC at the discharge station. The model then enabled the estimation of an active groundwater reservoir in the forefield. Based on the initial hypothesis of a superposition of two linear reservoirs, we found that the deeper reservoir empties slowly and has a volume equivalent to the area of the forefield (1000 by 400 m) with a depth of 1.7 m if porosity is assumed constant at 0.25. A shallower aquifer fills on top of the base aquifer during summer and responds rapidly to daily fluctuations in stream stage.

Geophysical campaigns have however shown that depth to bedrock is likely to be at least 10 m in most of the forefield (Kobierska, 2014). We can therefore expect part of the saturated sediment volume to act as a passive aquifer flowing below the discharge station. How much this hidden groundwater flow component affects the yearly water balance would be difficult to assess. Note that at the beginning of spring snowmelt recharge in 2011 (Fig. 5), modelling shows that the slow “active” reservoir had not completely emptied over the winter before recharge by snowmelt started.

### Linking baseflow separation in an alpine basin

F. Kobierska et al.

Title Page

Abstract

Introduction

Conclusions

References

Tables

Figures



Back

Close

Full Screen / Esc

Printer-friendly Version

Interactive Discussion



### 5.3 Limitations and uncertainties

One key problem with the use of mixing models in such an environment is the limited range of variation in EC. The recorded values are also at the lower end of what can be measured by typical instrumentation. However, the use of four years of data defined by strong and consistent daily fluctuations allowed for interesting findings. Brown (2002) highlights that mixing models are not as well adapted to glacial environments as previously thought. In our case, however, the length and high temporal resolution of the time series make the technique worth testing.

Considering hydrology in the forefield as the mixing of only two water sources is clearly a great simplification. We can list a total a four components: snowmelt, glacier melt, groundwater exfiltration, and rainwater. Rainfall is hard to quantify due to strong elevation gradients. Had rainfall been known, a three-component mixing model with a rain endmember of  $6.05 \mu\text{S cm}^{-1}$  (Table 2) would not have had a significant impact, since the average measured EC at the discharge station was  $6.6 \mu\text{S cm}^{-1}$ . For this reason, as well as the quick routing of rainwater through the catchment due to steep topography, the model performance did not significantly improve with further filtering of rainfall (see the modelling assumptions in Sect. 3.1).

Modelled groundwater exfiltration does not solely describe localized groundwater resurgence via springs. Quick hyporheic exchange must lead to some increase in stream water EC as water flows through the forefield. Those processes are considered as groundwater exfiltration by the model and may represent a significant fraction of groundwater flow in the forefield. Brutsaert (2005) stressed that characterizing a basin as a single lumped unit with basin scale parameters is a useful concept but has limitations. The heterogeneity between different sections of the aquifer is not taken into account, since the model considers the aquifer as a homogenous body. It is nonetheless noteworthy that our simple model, consisting of only two linear reservoirs and considering only two water sources, reliably predicted discharge. This suggests that despite its simplicity, the modelling approach provided an adequate description of the

HESSD

11, 12187–12221, 2014

## Linking baseflow separation in an alpine basin

F. Kobierska et al.

Title Page

Abstract

Introduction

Conclusions

References

Tables

Figures



Back

Close

Full Screen / Esc

Printer-friendly Version

Interactive Discussion



catchment's hydrogeology. The rugged topography and heterogeneous soils should lead to non-linear behaviors at a smaller scale. However, as pointed out by Fenicia et al. (2006), groundwater reservoirs at the catchment scale tend to show relatively simple behavior.

5 Distributed physically-based models could potentially yield better results, but they require reliable soil data at high spatial resolution. It is typically difficult or impossible in alpine catchments to gather such a wealth of data. Obtaining adequate snowmelt and glacier melt data alone presents modelling challenges, as described in previous works at this catchment (Magnusson et al., 2011; Kobierska et al., 2013).

## 10 5.4 Effect of snowmelt and sub-glacial glacier melt

Every year, the model tended to overestimate total discharge in mid-summer and underestimate at both ends of the season. At the beginning of the 2009 season (Fig. 3, zoom 1), for instance, discharge is clearly underestimated during high flow spells, whereas midAugust is more correctly modelled (Fig. 3, zoom 2). As mentioned in the results section, this deficiency is likely due to variations in the "glacier melt" EC end-member. In early summer, this component is actually mainly snowmelt. The difficulty is that snowmelt has a relatively slow release rate and is in direct contact with saturated ground. Snowmelt is thus more likely to infiltrate into soils than glacier melt, leading to intermediate EC values. This had been evidenced in earlier studies such as Sueker et al. (2000).

20 Peak discharge values were also under-estimated in autumn (Fig. 3, zoom 3). The glacier melt endmember may again have been slightly too small. According to Hindshaw et al. (2011), at the end of each season the formation of a thin snow cover on the glacier leads to sub-glacial routing of residual glacier melt, in contrast to the fast-flowing melt channels observed during summer (see Fig. 9 in Hindshaw et al., 2011).  
25 This implies longer residence times under the glacier, thereby increasing electrical conductivity and leading to underestimation of total discharge.

### Linking baseflow separation in an alpine basin

F. Kobierska et al.

Title Page

Abstract

Introduction

Conclusions

References

Tables

Figures



Back

Close

Full Screen / Esc

Printer-friendly Version

Interactive Discussion



Hindshaw et al. (2011) had focused on seasonal variations of the contribution of a “sub-glacial component”. They, however, termed stream water–groundwater exchanges under the “dead ice body” as sub-glacial, which in our context may be misleading. As mentioned above, we agree with their conclusions that the sub-glacial component changes behavior during the hydrological season. In our opinion, stream water–groundwater exchanges under the “dead ice body” affect stream water EC more than sub-glacial flow under the bulk of the glacier, which appears to lack a substantial underlying sediment layer.

### 5.5 Suggestions for future studies

Year-round availability of reliable groundwater level data would have been very useful to further test the robustness of this approach. One difficulty in defining the fast reservoir function was indeed the shallowness of most groundwater tubes. We lacked an absolute measure of storage during winter and the integral storage function had to be shifted so that the upper fast reservoir emptied to a low residual value at the end October. This is typically the end of the main hydrological season in high Alpine catchments. As mentioned in the methods, a small residual groundwater storage volume was added to the reservoir for the years that did not display pure recession from the slow reservoir at the end of the calibration period. Groundwater data usually became less reliable in November because potential icing or snow cover affected the atmospheric pressure compensation of the signal. For this reason, the storage calculation was stopped every year at the end of October.

In contrast to EC measurements, isotope ratios have the advantage of being fully conservative. But since the hydrological signal displays daily fluctuations, mixing models would require automated isotope sampling, infrastructure that is both fragile and expensive to install in such a site. Manual oxygen isotope samples (see  $\delta^{18}\text{O}$  values in Hindshaw et al., 2011) also showed that groundwater mainly consisted of glacier meltwater. Only in localized areas did heavier isotopes suggest some mixing with rainwater. However, at sites presenting stronger contrasts between rainwater, groundwater

## Linking baseflow separation in an alpine basin

F. Kobierska et al.

[Title Page](#)

[Abstract](#)

[Introduction](#)

[Conclusions](#)

[References](#)

[Tables](#)

[Figures](#)



[Back](#)

[Close](#)

[Full Screen / Esc](#)

[Printer-friendly Version](#)

[Interactive Discussion](#)









**Linking baseflow separation in an alpine basin**

F. Kobierska et al.

[Title Page](#)[Abstract](#)[Introduction](#)[Conclusions](#)[References](#)[Tables](#)[Figures](#)[⏪](#)[⏩](#)[◀](#)[▶](#)[Back](#)[Close](#)[Full Screen / Esc](#)[Printer-friendly Version](#)[Interactive Discussion](#)

- Magnusson, J., Farinotti, D., Jonas, T., and Bavay, M.: Quantitative evaluation of different hydrological modeling approaches in a partly glacierized Swiss watershed, *Hydrol. Process.*, 25, 2071–2084, doi:10.1002/hyp.7958, 2011.
- 5 Magnusson, J., Jonas, T., and Kirchner, J.: Temperature dynamics of a proglacial stream: identifying dominant energy balance components and inferring spatially integrated hydraulic geometry, *Water Resour. Res.*, 48, W06510, doi:10.1029/2011WR011378, 2012.
- Magnusson, J., Kobierska, F., Huxol, S., Hayashi, M., Jonas, T., and Kirchner, J. W.: Melt water driven stream and groundwater stage fluctuations on a glacier forefield (Damma gletscher, Switzerland), *Hydrol. Process.*, 28, 823–836, doi:10.1002/hyp.9633, 2014.
- 10 Majone, B., Bertagnoli, A., and Bellin, A.: A non-linear runoff generation model in small Alpine catchments, *J. Hydrol.*, 385, 300–312, doi:10.1016/j.jhydrol.2010.02.033, 2010.
- Rupp, D. E. and Selker, J. S.: On the use of the Boussinesq equation for interpreting recession hydrographs from sloping aquifers, *Water Resour. Res.*, 42, W12421, doi:10.1029/2006WR005080, 2006.
- 15 Rupp, D. E., Schmidt, J., Woods, R. A., and Bidwell, V. J.: Analytical assessment and parameter estimation of a low-dimensional groundwater model, *J. Hydrol.*, 377, 143–154, doi:10.1016/j.jhydrol.2009.08.018, 2009.
- Sueker, J. K., Ryan, J. N., Kendall, C., and Jarrett, R. D.: Determination of hydrologic pathways during snowmelt for alpine/subalpine basins, Rocky Mountain National Park, Colorado, *Water Resour. Res.*, 36, 63–75, 2000.
- 20 Weijs, S. V., Mutzner, R., and Parlange, M. B.: Could electrical resistivity replace water level in rating curves for alpine streams?, *Water Resour. Res.*, 49, 343–351, doi:10.1029/2012WR012181, 2013.
- Wittenberg, H. and Sivapalan, M.: Watershed groundwater balance estimation using streamflow recession analysis and baseflow separation, *J. Hydrol.*, 219, 20–33, 1999.
- 25



## Linking baseflow separation in an alpine basin

F. Kobierska et al.

**Table 2.** Results of EC measurements ( $\mu\text{S cm}^{-1}$ ) in the forefield. The zones refer to those drawn in Figs. 1 and 6.

Zone	Average	Min	Max	SD	No. of samples
H1	15.5	12.8	18.3	1.2	89
H2	12.7	10.9	14	1.2	15
H3	15.4	13.6	17.8	1.3	13
H1+H2+H3	15.1	10.9	18.3	1.5	117
Rain	6.1	4.3	7.5	1.3	4

[Title Page](#)
[Abstract](#)
[Introduction](#)
[Conclusions](#)
[References](#)
[Tables](#)
[Figures](#)

[Back](#)
[Close](#)
[Full Screen / Esc](#)
[Printer-friendly Version](#)
[Interactive Discussion](#)




## Linking baseflow separation in an alpine basin

F. Kobierska et al.

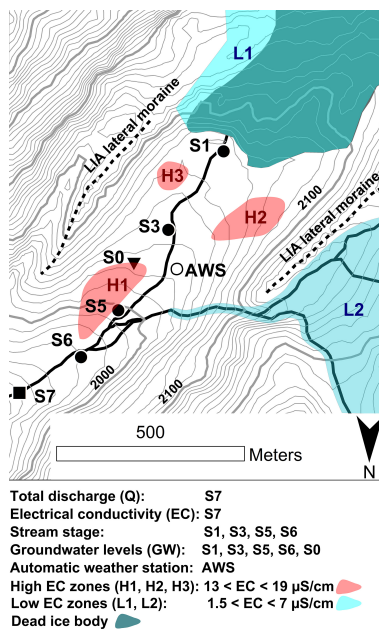


**Figure 1.** The Damma glacier forefield: at sites S1, S3, S5 and S6 (solid circles), stream and groundwater levels are recorded. At site S7 (solid square), stream stage is measured for total discharge. At site S0 (solid triangle), only one groundwater tube is installed. Color patches indicate zones of high (H1, H2 and H3) and low (L1, L2) electrical conductivity. An automatic weather station (AWS) is located in the middle of the forefield. Lateral moraines are indicated with dashed black lines and terrain elevation is shown by 10 m contour intervals. (Figure adapted from Magnusson et al., 2014).

Title Page

Abstract

Introduction

Conclusions

References

Tables

Figures



Back

Close

Full Screen / Esc

Printer-friendly Version

Interactive Discussion



## Linking baseflow separation in an alpine basin

F. Kobierska et al.

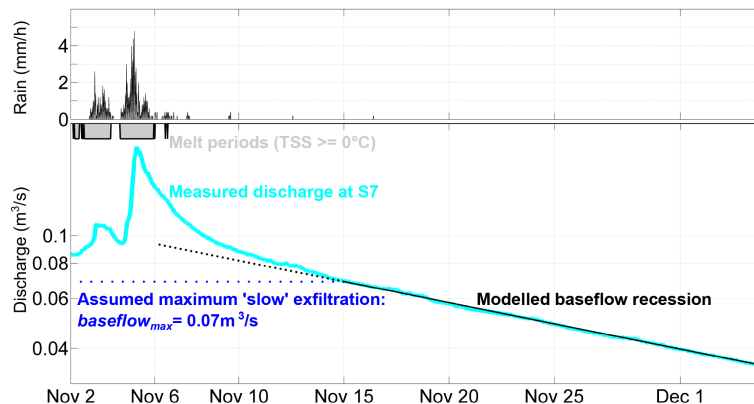


**Figure 2.** Baseflow recession during November 2008. The lower panel shows measured and modelled discharge at S7 on a logarithmic scale. The dotted black line illustrates how the modelled baseflow recession diverges from measured discharge before 15 November. Note that melting periods (non-negative temperature of snow surface) are indicated as grey shaded bars. The upper panel plots successive rain events.

[Title Page](#)[Abstract](#)[Introduction](#)[Conclusions](#)[References](#)[Tables](#)[Figures](#)[⏪](#)[⏩](#)[⏴](#)[⏵](#)[Back](#)[Close](#)[Full Screen / Esc](#)[Printer-friendly Version](#)[Interactive Discussion](#)





## Linking baseflow separation in an alpine basin

F. Kobierska et al.

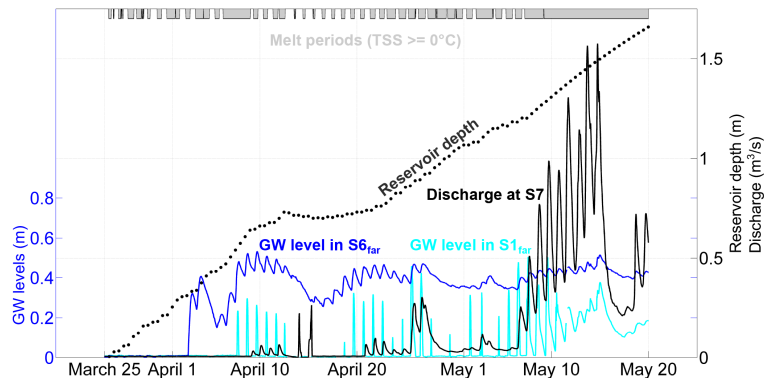


**Figure 5.** Recharge of the slow reservoir from snowmelt in spring 2011. Snow melt periods (non-negative snow surface temperature) are indicated as grey shading. Groundwater levels, displayed in blue, represent the depth of water in each tube. Total discharge and reservoir depth are plotted in black. Reservoir depth is computed based on a surface area of 400 by 1000 m.

[Title Page](#)[Abstract](#)[Introduction](#)[Conclusions](#)[References](#)[Tables](#)[Figures](#)[Back](#)[Close](#)[Full Screen / Esc](#)[Printer-friendly Version](#)[Interactive Discussion](#)

